Quantum effects in energy and charge transfer in an artificial photosynthetic complex

Pulak Kumar Ghosh,[1,a)] Anatoly Yu. Smirnov,[1,2] and Franco Nori[1,2]

[1]*Advanced Science Institute, RIKEN, Wako, Saitama 351-0198, Japan*
[2]*Physics Department, The University of Michigan, Ann Arbor, Michigan 41109-1040, USA*

We investigate the quantum dynamics of energy and charge transfer in a wheel-shaped artificial photosynthetic antenna-reaction center complex. This complex consists of six light-harvesting chromophores and an electron-acceptor fullerene. To describe quantum effects on a femtosecond time scale, we derive the set of exact non-Markovian equations for the Heisenberg operators of this photosynthetic complex in contact with a Gaussian heat bath. With these equations we can analyze the regime of strong system-bath interactions, where reorganization energies are of the order of the intersite exciton couplings. We show that the energy of the initially excited antenna chromophores is efficiently funneled to the porphyrin-fullerene reaction center, where a charge-separated state is set up in a few picoseconds, with a quantum yield of the order of 95%. In the single-exciton regime, with one antenna chromophore being initially excited, we observe quantum beatings of energy between two resonant antenna chromophores with a decoherence time of ~100 fs. We also analyze the double-exciton regime, when two porphyrin molecules involved in the reaction center are initially excited. In this regime we obtain pronounced quantum oscillations of the charge on the fullerene molecule with a decoherence time of about 20 fs (at liquid nitrogen temperatures). These results show a way to directly detect quantum effects in artificial photosynthetic systems. © *2011 American Institute of Physics*. [doi:10.1063/1.3600341]

I. INTRODUCTION

The multistep energy-transduction process in natural photosystems begins with capturing sunlight photons by light-absorbing antenna chromophores surrounding a reaction center.[1,2] The antenna chromophores transfer radiation energy to the reaction center directly or through a series of accessory chromophores. The reaction center harnesses the excitation energy to create a stable charge-separated state.

Energy transfer in natural and artificial photosynthetic structures has been an intriguing issue in quantum biophysics due to the conspicuous presence of long-lived quantum coherence observed with two-dimensional Fourier transform electronic spectroscopy.[3,4] These experimental achievements have motivated researchers to investigate the role of quantum coherence in very efficient energy transmission, which takes place in natural photosystems.[5–9] Quantum coherent effects surviving up to room temperatures have also been observed in artificial polymers.[10] Artificial photosynthetic elements, mimicking natural photosystems, might serve as building blocks for efficient and powerful sources of energy.[11,12] Some of these elements have been created and studied experimentally in Refs. 13–18. The theoretical modelling of artificial reaction centers has been recently performed in Refs. 19 and 20.

Here, we study energy transfer and charge separation in a wheel-shaped molecular complex (BPF complex, see Fig. 1) mimicking a natural photosynthetic system. This complex has

been synthesized and experimentally investigated in Ref. 17. It has four antennas – two bis(phenylethynyl)anthracene (BPEA) molecules and two borondipyrromethene (BDPY) chromophores, as well as two zinc porphyrins (ZnPy$_a$ and ZnPy$_b$). These six light-absorbing chromophores are attached to a central hexaphenylbenzene core. Electrons can tunnel from the zinc porphyrin molecules to a fullerene F (electron acceptor). Thus, two porphyrins and the fullerene molecule form an artificial reaction center (ZnPy$_a$-F-ZnPy$_b$). The BPEA chromophores strongly absorb around 450 nm (the blue region), while the BDPY moieties have good absorptions around 513 nm (green region). Porphyrins have absorption peaks at both red and orange wavelengths. Therefore, the BPF complex can utilize most of the rainbow of sunlight – from blue to red photons. It is shown in Ref. 17 that the absorption of photons results in the formation of a porphyrin-fullerene charge-separated state with a lifetime of 230 ps; in doing so, excitations from the BPEA and BDPY antenna chromophores are transferred to the porphyrins with a subsequent donation of an electron from the excited states of the porphyrins to the fullerene moiety. This process takes a few picoseconds, suggesting that the excitonic coupling between chromophores is sufficiently strong. The electronic coupling between the porphyrins and the fullerene controlling tunneling of electrons in the artificial reaction center also should be quite strong. It should be noted, however, that spectroscopic data[15–17] show that the absorption spectrum of the BPF complex is approximately represented as a superposition of contributions from the individual chromophores with almost no perturbations due to the links between the chromophores. This means that the chromophores comprising the light-harvesting complex can

a)Author to whom correspondence should be addressed. Electronic mail:
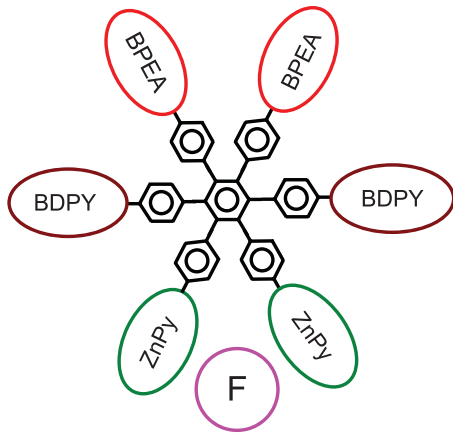pulak@riken.jp.

134, 244103-1

FIG. 1. Schematic diagram of the wheel-shaped artificial antenna-reaction center complex reported in Ref. 17. We use the short notation, *BPF complex*, to denote this photosynthetic device. The antenna-reaction center complex contains six light-harvesting pigments: (i) two bis(phenylethynyl)anthracene chromophores, $BPEA_a$ and $BPEA_b$, (ii) two borondipyrromethene chromophores, $BDPY_a$ and $BDPY_b$, and (iii) two zinc tetraarylporphyrin chromophores, $ZnPy_a$ and $ZnPy_b$. All the chromophores are attached to a rigid hexaphenyl benzene core. In addition to the antenna components, the photosystem contains a fullerene derivative (F) containing two pyridyl groups, acting as an electron acceptor. The fullerene derivative F is attached to the both ZnPy chromophores via the coordination of the pyridyl nitrogens with the zinc atoms. For structural details of the BPF complex, we refer to Refs. 17 and 28.

be considered as individual interacting units, but not as an extended single chromophore. We can expect that, at these conditions, quantum coherence is able to play an important role in energy and charge-transfer dynamics, manifesting itself in quantum beatings of chromophore populations as well as in quantum oscillations of the charge accumulated on the fullerene molecule. In principle, these oscillations could be measured by a sensitive single-electron transistor, thus providing a direct proof of quantum behavior in the artificial photosynthetic complex. Since these phenomena occurs at very short time scales (a few femtoseconds), they could be within the reach of femtosecond spectroscopy in the near future. The main goal of this study is to explore quantum features of the energy and charge transfer in a wheel-shaped antenna-reaction center complex at subpicosecond time scales.

II. MODEL AND METHODS

A. Hamiltonian

Each chromophore has one ground and one excited state, whereas the electron-acceptor fullerene F has just one energy level with energy E_F. We introduce creation (annihilation) operators, $a_k^\dagger$ (a_k), of an electron on the kth site. The electron population operators are defined as $n_k = a_k^\dagger a_k$. We assume that each electron state can be occupied by a single electron, as spin degrees of freedom are neglected. The basic Hamiltonian of the system has the form

$$H_0 = \sum_k (E_k n_k + E_{k^*} n_{k^*}) + E_F n_F + H_C$$
$$+ \sum_{k \neq l} V_{kl} a_{k^*}^\dagger a_k \, a_l^\dagger a_{l^*} - \sum_{\sigma\sigma'} \Delta_{\sigma\sigma'} a_\sigma^\dagger a_{\sigma'}, \quad (1)$$

where the first part incorporates the energies of the electron states (hereafter $k, l = BPEA_a$, $BPEA_b$, $BDPY_a$, $BDPY_b$, $ZnPy_a$, $ZnPy_b$), and the second term is related to a fullerene energy level E_F with a population operator $n_F = a_F^\dagger a_F$. The pair (k, k^*) denotes a ground (k) and an excited (k^*) state of an electron located on the site k with the corresponding energy E_k (E_{k^*}). The term H_C represents the contribution of Coulomb interactions between electron-binding sites. This term is given in Appendix A. The fourth term of Eq. (1) describes excitonic couplings between the chromophores k and l. The matrix element V_{kl} is a measure of an interchromophoric coupling strength. The last term in Eq. (1) describes the electron tunneling from excited states of the porphyrin molecules ($ZnPy_a$ and $ZnPy_b$) to the electron-acceptor F characterized by the tunneling amplitudes $\Delta_{\sigma\sigma'}$, where σ, $\sigma' = ZnPy_a^*$, $ZnPy_b^*$, F.

The interaction of the system with the environment (heat bath), represented here by a sum of independent oscillators with Hamiltonian

$$H_{env} = \sum_j \left(\frac{p_j^2}{2m_j} + \frac{m_j \omega_j^2 x_j^2}{2} \right), \quad (2)$$

is given by the term

$$H_{e-ph} = -\sum_{jk} m_j \omega_j^2 x_{jk} x_j n_k, \quad (3)$$

where x_j and p_j are the position and momentum of the jth oscillator having an effective mass m_j and a frequency ω_j. The coefficients x_{jk} define the strength of the coupling between the electron subsystem and the environment.

The contribution of the energy-quenching mechanisms responsible for the recombination processes in the system is given by the Hamiltonian,

$$H_{quen} = -\sum_l (q_l^\dagger a_{l^*}^\dagger a_l + q_l a_l^\dagger a_{l^*}). \quad (4)$$

For the sake of simplicity, we include the radiation damping of the excited states into the energy-quenching operator q_l. The first term in the Hermitian Hamiltonian H_{quen} is related to the excitation of the l-chromophore by the quenching bath, whereas the second term corresponds to the reverse process, namely, to the absorption of chromophore energy by the bath. Both processes are necessary to provide correct conditions for the thermodynamic equilibrium between the system and the bath.

The total Hamiltonian of the system is

$$H = H_0 + H_{e-ph} + H_{env} + H_{quen}. \quad (5)$$

We omit here the Hamiltonian of the quenching (radiation) heat bath.

B. Diagonalization of H_0

We choose 160 basis states $|M\rangle$ of the complex including a vacuum state, where all chromophores are in the ground state and the F site is empty. We diagonalize the Hamiltonian H_0 in Eq. (1) to consider the case where the excitonic coupling between chromophores, described by coefficients V_{lm},

and the porphyrin-fullerene tunneling, which is determined by amplitudes $\Delta_{\sigma\sigma'}$, cannot be analyzed within perturbation theory. In the new basis, $|\mu\rangle = \sum_M |M\rangle\langle M|\mu\rangle$, the Hamiltonian H_0 is diagonal with the energy spectrum $\{E_\mu\}$, so that the total Hamiltonian of the system H has the form

$$H = \sum_\mu E_\mu |\mu\rangle\langle\mu| - \sum_{\mu\nu} \mathcal{A}_{\mu\nu}|\mu\rangle\langle\nu| + H_{\text{env}}. \tag{6}$$

Here

$$\mathcal{A}_{\mu\nu} = Q_{\mu\nu} + q_{\mu\nu} \tag{7}$$

is the combined operator for both heat baths with fluctuating in time variables:

$$Q_{\mu\nu} = \sum_j m_j \omega_j^2 x_j [x_{jF}\langle\mu|n_F|\nu\rangle$$

$$+ \sum_k (x_{jk}\langle\mu|n_k|\nu\rangle + x_{jk*}\langle\mu|n_{k*}|\nu\rangle)], \tag{8}$$

$$q_{\mu\nu} = \sum_l \langle\mu|a_l^\dagger a_{l*}|\nu\rangle q_l + \text{H.c.} \tag{9}$$

To distinguish the processes of energy transfer, where the number of electrons on each chromophore remains constant, from the processes of charge transfer, where the total population of the site changes, we introduce the following operators:

$$S_l = n_l + n_{l*}, \quad M_l = n_l - n_{l*}, \tag{10}$$

together with coefficients

$$\bar{x}_{jl} = \frac{x_{jl} + x_{jl*}}{2}, \qquad \tilde{x}_{jl} = \frac{x_{jl} - x_{jl*}}{2}. \tag{11}$$

Thus, the environment operator $Q_{\mu\nu}$ can be rewritten as

$$Q_{\mu\nu} = \sum_j m_j \omega_j^2 x_j \Lambda_j^{\mu\nu}, \tag{12}$$

with

$$\Lambda_j^{\mu\nu} = \sum_l \{\bar{x}_{jl}\langle\mu|S_l|\nu\rangle + \tilde{x}_{jl}\langle\mu|M_l|\nu\rangle\} + x_{jF}\langle\mu|n_F|\nu\rangle. \tag{13}$$

C. Non-Markovian equations for the system operators

An arbitrary electron operator W can be expressed in terms of the basic operators $\rho_{\mu\nu} = |\mu\rangle\langle\nu|$; with $W = \sum_{\mu\nu} W_{\mu\nu}\rho_{\mu\nu}$, and $W_{\mu\nu} = \langle\mu|W|\nu\rangle$. The operator $\rho_{\mu\nu}$ denotes a matrix with zero elements, with the exception of the single element at the crossing of the μ-row and the ν-column. The matrix elements $W_{\mu\nu}$ of any electron operator can be easily calculated (see, e.g., Eqs. (S10) and (S11) in the supplementary material for Ref. 20). For example, an electron localized in a two-well potential,[21] with the right and left states $|1\rangle$ and $|2\rangle$, is described by the Pauli matrices $\{\sigma_x, \sigma_y, \sigma_z\}$: $\sigma_z = |1\rangle\langle1| - |2\rangle\langle2|$, $\sigma_x = |1\rangle\langle2| + |2\rangle\langle1|$, and $\sigma_y = i(|2\rangle\langle1| - |1\rangle\langle2|)$, which are expressed in terms of the basic operators $|\mu\rangle\langle\nu|$ with $\mu, \nu = 1, 2$.

In the Heisenberg picture, the operator W evolves in time according to the equation: $i(\partial W/\partial t) = [W, H]_-$. This evolution can be described with the time-evolving operators, $\rho_{\mu\nu}(t) = (|\mu\rangle\langle\nu|)(t)$, which satisfy the Heisenberg equation:

$$i\frac{\partial\rho_{\mu\nu}}{\partial t} = [\rho_{\mu\nu}, H]_- = -\omega_{\mu\nu}\rho_{\mu\nu} - \sum_\alpha (\mathcal{A}_{\nu\alpha}\rho_{\mu\alpha} - \mathcal{A}_{\alpha\mu}\rho_{\alpha\nu}),$$

$$\tag{14}$$

where $\omega_{\mu\nu} = E_\mu - E_\nu$, and the heat-bath operator $\mathcal{A}_{\mu\nu}$ is defined in Eq. (7). Here, we use the fact that the Hamiltonian H in Eq. (6) is also expressed in terms of the operators $\rho_{\mu\nu}$ taken at the same moment of time t. For two of these operators, $\rho_{\mu\nu}(t)$ and $\rho_{\alpha\beta}(t)$, we have simple multiplication rules: $\rho_{\mu\nu}\rho_{\alpha\beta} = \delta_{\nu\alpha}\rho_{\mu\beta}$. These rules allow to calculate commutators of basic operators taken at the same moment of time. We note that at the initial moment of time the operator, $\rho_{\mu\nu}(0) \equiv |\mu\rangle\langle\nu|$, is represented by the above-mentioned zero matrix with a single unit at the μ-ν intersection. The matrix elements of the electron operators in Eqs. (9) and (13) are taken over the time-independent eigenstates of the Hamiltonian H_0. The bath operators $\mathcal{A}_{\mu\nu}$ fluctuate in time since they depend on the environmental variables, $\{x_j(t)\}$, and on the variables $\{q_l(t)\}$ of the quenching bath.

It is known that the dissipative evolution of the two-state system can be described by the Heisenberg equations for the Pauli matrices $\{\sigma_x, \sigma_y, \sigma_z\}$ with the spin-boson Hamiltonian [see Eq. (1.4) in Ref. 21], which includes environmental degrees of freedom. The artificial photosynthetic complex analyzed in the present paper has 160 states. A dissipative evolution of this complex is described by the Hamiltonian H in Eq. (6), written in terms of the Heisenberg operators $\rho_{\mu\nu}(t) = (|\mu\rangle\langle\nu|)(t)$ taken at the moment of time t. Instead of the time-dependent Pauli matrices, the time evolution of the two-state dissipative system can be described by the basic operators $|1\rangle\langle1|$, $|1\rangle\langle2|$, $|2\rangle\langle1|$, $|2\rangle\langle2|$, evolving in time. In a similar manner,[22] the evolution of the multi-state photosynthetic complex is described by the set of the time-dependent Heisenberg operators $\rho_{\mu\nu}(t)$, which obey Eq. (14). As its spin-boson counterpart, the Hamiltonian H in Eq. (6) contains the Hamiltonian, H_{env}, of the heat-bath as well as the system-bath interaction terms. Here, we generalize the spin-boson model from the case of two states to the case of 160 states. With a knowledge of the operators $\rho_{\mu\nu}(t)$, it is possible to find the time evolution of any Heisenberg operator of the system. Only at the initial moment of time, $t = 0$, the operators $\rho_{\mu\nu}(0)$ form the basis of the Liouville space. Note that we work in the Heisenberg representation, without using the description based on the von Neumann equations for the density matrix.

To obtain functions that can be measured in experiments, we have to average the operator $\rho_{\mu\nu}(t)$ and Eq. (14) over the initial state $|\Psi^0\rangle$ of the electron subsystem as well as over the Gaussian distribution, $\rho_T = \exp(-H_{\text{bath}}^{(0)}/T)$, of the equilibrium bath, $\langle\ldots\rangle_T$, with temperature T and with a free Hamiltonian $H_{\text{bath}}^{(0)}$, which comprises the free environment Hamiltonian and the free Hamiltonian of the quenching bath. The notation $\langle\ldots\rangle$ means double averaging:

$$\langle\ldots\rangle = \langle\langle\Psi^0|\ldots|\Psi^0\rangle\rangle_T. \tag{15}$$

The quantum-mechanical average value of the initial basic matrix, $\langle \Psi^0 | \rho_{\mu\nu}(0) | \Psi^0 \rangle = \langle \Psi^0 | \mu \rangle \langle \nu | \Psi^0 \rangle$, is determined by the product of amplitudes to find the electron subsystem at the initial moment of time in the eigenstates $|\mu\rangle$ and $|\nu\rangle$ of the Hamiltonian H_0.

A standard density matrix, $\bar{\rho} = \{\bar{\rho}_{\mu\nu}\}$, of the electron subsystem is a deterministic function which allows to calculate the average value of an arbitrary operator W with the formula:

$$\langle W(t) \rangle = Tr[\bar{\rho}(t) W] = \sum_{\mu\nu} W_{\mu\nu} \bar{\rho}_{\nu\mu}(t). \quad (16)$$

The same average value can be written as $\langle W(t) \rangle = \sum_{\mu\nu} W_{\mu\nu} \langle \rho_{\mu\nu}(t) \rangle$, which means that the average matrix, $\langle \rho_{\mu\nu}(t) \rangle = \bar{\rho}_{\nu\mu}(t)$, has matrix elements related to the transposed density matrix $\bar{\rho}(t)$.

It should be emphasized that the time evolution of the heat-bath operators $\{x_j, \, p_j\}$ and $\{q_l\}$, as well as their linear combinations $Q_{\mu\nu}$, $q_{\mu\nu}$, and $\mathcal{A}_{\mu\nu}$, are determined by the total Hamiltonian H in Eq. (6). In the absence of an interaction with the dynamical system (the electron-binding sites), the free-phonon operators $Q_{\mu\nu}^{(0)}$, as well as the free operators of the other baths, $q_{\mu\nu}^{(0)}$, are described by Gaussian statistics,[23] as in the case of an environment comprising independent linear oscillators with the Hamiltonian H_{env} in Eq. (2). Using Gaussian property, Efremov et al.[24] derived non-Markovian Heisenberg–Langevin equations, without using perturbation theory, that assumes a weak system-bath interaction. Recently, a similar non-perturbative approach has been developed by Ishizaki and Fleming in Ref. 25. Due to Gaussian properties of the free bath, the total operator $\mathcal{A}_{\mu\nu}$ of the combined dissipative environment is a linear functional of the operators $\rho_{\mu\nu}$,

$$\mathcal{A}_{\mu\nu}(t) = \mathcal{A}_{\mu\nu}^{(0)}(t)$$
$$+ \sum_{\bar{\mu}\bar{\nu}} \int dt_1 \langle i [\mathcal{A}_{\mu\nu}^{(0)}(t), \mathcal{A}_{\bar{\mu}\bar{\nu}}^{(0)}(t_1)]_- \rangle \theta(t - t_1) \rho_{\bar{\mu}\bar{\nu}}(t_1), \quad (17)$$

where $\theta(\tau)$ is the Heaviside step function. We note that this expansion directly follows from the solution of the Heisenberg equations for the positions $\{x_j\}$ and $\{q_l\}$ of the bath oscillators. It is shown in Ref. 24 that the average value of the free operator $\mathcal{A}_{\mu\nu}^{(0)}(t)$ multiplied by an arbitrary operator $\mathcal{B}(t)$ is proportional to the functional derivative of the operator $\mathcal{B}$ over the variable $\mathcal{A}_{\mu\nu}^{(0)}(t)$:

$$\langle \mathcal{A}_{\mu\nu}^{(0)}(t) \mathcal{B}(t) \rangle = \sum_{\bar{\mu}\bar{\nu}} \int dt_1 \langle \mathcal{A}_{\mu\nu}^{(0)}(t) \mathcal{A}_{\bar{\mu}\bar{\nu}}^{(0)}(t_1) \rangle \times \left\langle \frac{\delta \mathcal{B}(t)}{\delta \mathcal{A}_{\bar{\mu}\bar{\nu}}^{(0)}(t_1)} \right\rangle, \quad (18)$$

with

$$\frac{\delta \mathcal{B}(t)}{\delta \mathcal{A}_{\bar{\mu}\bar{\nu}}^{(0)}(t_1)} = i [\mathcal{B}(t), \rho_{\bar{\mu}\bar{\nu}}(t_1)]_- \, \theta(t - t_1). \quad (19)$$

Substituting Eqs. (17)–(19) into Eq. (14) we derive the exact non-Markovian equation for the Heisenberg operators $\rho_{\mu\nu}$ of the dynamical system (chromomorphic sites + fullerene)

interacting with a Gaussian heat bath,

$$\langle \dot{\rho}_{\mu\nu} \rangle - i \, \omega_{\mu\nu} \langle \rho_{\mu\nu} \rangle = \sum_{\alpha\bar{\mu}\bar{\nu}} \int_0^t dt_1 \{ \langle \mathcal{A}_{\bar{\mu}\bar{\nu}}^{(0)}(t_1) \mathcal{A}_{\nu\alpha}^{(0)}(t) \rangle \langle \rho_{\bar{\mu}\bar{\nu}}(t_1) \rho_{\mu\alpha}(t) \rangle$$
$$- \langle \mathcal{A}_{\nu\alpha}^{(0)}(t) \mathcal{A}_{\bar{\mu}\bar{\nu}}^{(0)}(t_1) \rangle \langle \rho_{\mu\alpha}(t) \rho_{\bar{\mu}\bar{\nu}}(t_1) \rangle$$
$$+ \langle \mathcal{A}_{\alpha\mu}^{(0)}(t) \mathcal{A}_{\bar{\mu}\bar{\nu}}^{(0)}(t_1) \rangle \langle \rho_{\alpha\nu}(t) \rho_{\bar{\mu}\bar{\nu}}(t_1) \rangle$$
$$- \langle \mathcal{A}_{\bar{\mu}\bar{\nu}}^{(0)}(t_1) \mathcal{A}_{\alpha\mu}^{(0)}(t) \rangle \langle \rho_{\bar{\mu}\bar{\nu}}(t_1) \rho_{\alpha\nu}(t) \rangle \}. \quad (20)$$

The time evolution of the average operator $\langle \rho_{\mu\nu} \rangle$ is determined by the second-order correlation functions of the system operators as well as by the correlation functions of the free dissipative environment. Here, we do not impose any restrictions on the spectrum of the environment. It should be emphasized that the exact non-Markovian equation (20) goes far beyond the von Neumann equation, $i \dot{\bar{\rho}} = [H, \bar{\rho}]_-$, for the density matrix $\bar{\rho}$ of the electron subsystem.

D. Beyond the system-bath perturbation theory

We assume that the coupling of the system to the quenching heat bath determined by the Hamiltonian H_{quen} in Eq. (4) is weak enough to be analyzed perturbatively. However, an interaction of the chromophores with the protein environment cannot be treated entirely within perturbation theory since the reorganization energies are of the order of the intersite couplings. As in the theory of modified Redfield equations,[26,27] the phonon operator $Q_{\mu\nu}$ in Eq. (12) can be represented as a sum of diagonal $Q_\mu = Q_{\mu\mu}$ and off-diagonal $\tilde{Q}_{\mu\nu}$ parts:

$$Q_{\mu\nu} = Q_\mu \delta_{\mu\nu} + (1 - \delta_{\mu\nu}) \tilde{Q}_{\mu\nu}. \quad (21)$$

We derive equations for diagonal and off-diagonal elements of the matrix $\langle \rho_{\mu\nu}(t) \rangle$ (see Appendix B for details about the derivation), where the interaction with the off-diagonal elements of the environment operators $\tilde{Q}_{\mu\nu}$ are considered within the perturbation theory, and the effects of the diagonal elements Q_μ are treated exactly.

The time dependence of the electron distribution $\langle \rho_\mu \rangle$ (diagonal elements) over eigenstates of the Hamiltonian H_0 is governed by the equation

$$\langle \dot{\rho}_\mu \rangle + \gamma_\mu \langle \rho_\mu \rangle = \sum_\alpha \gamma_{\mu\alpha} \langle \rho_\alpha \rangle, \quad (22)$$

where the relaxation matrix $\gamma_{\mu\alpha}$ contains a contribution, $\tilde{\gamma}_{\mu\alpha}$, from the non-diagonal environment operators [see Eq. (B22)] as well as a contribution from the quenching processes, $\gamma_{\mu\alpha}^{quen}$ [see Eq. (B30)],

$$\gamma_{\mu\alpha} = \tilde{\gamma}_{\mu\alpha} + \gamma_{\mu\alpha}^{quen}, \quad (23)$$

with the total relaxation rate $\gamma_\mu = \sum_\alpha \gamma_{\alpha\mu}$. The time evolution of the off-diagonal elements are given by Eq. (B31) in Appendix B.

Equations (22) and (B31) allow us to determine the time evolution of an average value for an arbitrary operator W of the system: $\langle W(t) \rangle = \sum_{\mu\nu} \langle \mu | W | \nu \rangle \langle \rho_{\mu\nu}(t) \rangle$.

III. ENERGIES AND OTHER PARAMETERS

A. Energy levels and electrochemical potentials

The energies of the excited states of chromophores BPEA, BDPY, and ZnPy, in the BPF complex are estimated from the average between the longest wavelength absorption band and the shortest wavelength emission band of the chromophores. The average excited state energies of the chromophores BPEA, BDPY, and ZnPy are 2610 meV, 2370 meV, and 2030 meV, respectively, if we count from the corresponding ground energy levels.[16,17] Cyclic voltammetric studies[17] of reduction potentials with respect to the standard calomel electrode show that the first reduction potential of the fullerene derivative, F, is about -0.62 V and the first oxidation potential of ZnPy is about 0.75 V. From these data we calculate that the energy of the charge-separated state $ZnPy^+ - F^-$ is about 1370 meV. This energy is the sum of the energy of an electron on site F and the Coulomb interaction energy between a positive charge on ZnPy and a negative charge on F. The Coulomb energy can be calculated with the formula $u = e^2/4\pi\epsilon_0\epsilon r$, where ϵ_0 is the vacuum dielectric constant. The dielectric constant ϵ of 1,2-difluorobenzene (a solvent used in all experimental measurements of Ref. 17) is about 13.8. If the distance r between porphyrin ZnPy and fullerene F is about 1 nm, the Coulomb interaction energy is about 105 meV. Thus, the estimated energy of the electron on F can be of the order of 1475 meV.

B. Reorganization energies and coupling strengths

The reorganization energies for exciton and electron transfer processes and electronic coupling strengths between the chromophores depend on the mutual distances and orientations of the components, strengths of chemical bonds, solvent polarity, and other structural details of the system. Precise values of these parameters are not available. However, time constants for energy transfer between different chromophores in the BPF complex, as well as rates for transitions of electrons between the fullerene F and porphyrin chromophores ZnPy, have been reported in Ref. 17. We fit

TABLE II. Comparison between the calculated values of the time constants (using the parameter sets I and II) to the experimental values reported in Ref. 17.

Process	τ (Set I)	τ (Set II)	τ (Experimental)
$BPEA_a \rightarrow BPEA_b$, $BPEA_b \rightarrow BPEA_a$	$\sim$0.4 ps	$\sim$0.2 ps	0.4 ps
$BPEA_a \rightarrow BDPY_a$, $BPEA_b \rightarrow BDPY_b$	$\sim$5 ps	$\sim$5.4 ps	5–13 ps
$BDPY_a \rightarrow ZnPy_a$, $BDPY_b \rightarrow ZnPy_b$	$\sim$5 ps	$\sim$3.9 ps	2–15 ps
$BPEA_a \rightarrow ZnPy_a$, $BPEA_b \rightarrow ZnPy_b$	$\sim$12 ps	$\sim$12 ps	7 ps
$BPEA_b \rightarrow ZnPy_a$, $BPEA_a \rightarrow ZnPy_b$	$\sim$10 ps	$\sim$12 ps	6 ps
$ZnPy_b \rightarrow F$, $ZnPy_a \rightarrow F$	$\sim$3 ps	$\sim$3 ps	3 ps

the experimental values of these time constants with the rates following from our equations with the goal of extracting reasonable values for the reorganization energies and the electronic and excitonic couplings. In principle, many combinations of reorganization energies and coupling constants could be possible. For the sake of simplicity, we consider two sets of parameters, for two limiting situations. One parameter set (denoted by set I in Table I) corresponds to a larger excitonic couplings, V, compared to the reorganization energies, Λ, whereas another set of parameters (denoted by set II in Table I) considers the opposite case, where the reorganization energies are larger than the excitonic couplings. These two sets of parameters are presented in Table I. In addition to the parameters listed in Table I, we consider the following values for the charge-transfer reorganization energies (set I): $\lambda_F = 200$ meV, $\lambda_{lM} = 100$ meV, and $\lambda_F = 230$ meV, $\lambda_{lM} = 120$ meV (set II), where $l = ZnPy_a, ZnPy_b$. The values of the reorganization energies for energy-transfer processes are much smaller than those for charge transfer.

References 17 and 28 reported a very fast electron transfer (with a time constant $\tau \sim 3$ ps) between excited states of zinc porphyrins ($ZnPy_a, ZnPy_b$) and the fullerene derivative F. This fact indicates a good porphyrin-fullerene

TABLE I. Chosen values of the excitonic couplings (V) and reorganization energies for energy transfer (Λ) of the six antenna chromophores. We choose two sets of parameters, one set (denoted by I) corresponds to $V > \Lambda$ and the other set (II) to the opposite limit $V < \Lambda$. The calculated values of the time constants using both sets of parameters agree with the experimental values.

Chromophores	Set I		Set II	
	Coupling (V)	Reorganization energy (Λ)	Coupling (V)	Reorganization energy (Λ)
$BPEA_a \leftrightarrow BPEA_b$, $BPEA_b \leftrightarrow BPEA_a$	50 meV	$\Lambda_{BPEA_a} = 20$ meV $\Lambda_{BPEA_b} = 20$ meV	30 meV	$\Lambda_{BPEA_a} = 40$ meV $\Lambda_{BPEA_b} = 40$ meV
$BPEA_a \leftrightarrow BDPY_a$, $BPEA_b \leftrightarrow BDPY_b$	30 meV	$\Lambda_{BDPY_a} = 15$ meV $\Lambda_{BDPY_b} = 15$ meV	17 meV	$\Lambda_{BDPY_a} = 30$ meV $\Lambda_{BDPY_b} = 30$ meV
$BDPY_a \leftrightarrow ZnPy_a$, $BDPY_b \leftrightarrow ZnPy_b$	60 meV	$\Lambda_{ZnPy_a} = 20$ meV $\Lambda_{ZnPy_b} = 20$ meV	25 meV	$\Lambda_{ZnPy_a} = 40$ meV $\Lambda_{ZnPy_b} = 40$ meV
$BPEA_a \leftrightarrow ZnPy_a$, $BPEA_b \leftrightarrow ZnPy_b$	50 meV	...	40 meV	...
$BPEA_b \leftrightarrow ZnPy_a$, $BPEA_a \leftrightarrow ZnPy_b$	60 meV	...	40 meV	...

electronic coupling, which is due to the short covalent linkage and close spatial arrangement of the components.[28] Hereafter, we assume that the ZnPy-F tunneling amplitudes Δ are about 100 meV (parameter set I) and 80 meV (parameter set II). These parameters provide a quite fast electron transfer despite a significant energy gap between the ZnPy excited states and the fullerene energy level.

Using the parameter sets I and II we have calculated time constants for energy and charge processes. A comparison between the calculated and experimental values of the time constants has been presented in Table II.

To describe recombination processes, we introduce a coupling of the lth chromophore to a quenching heat bath characterized for simplicity by the Ohmic spectral density: $\chi_l''(\omega) = \alpha_l \omega$ with a dimensionless constant α_l. We assume that the shifts of the energy levels caused by the quenching bath are included into the renormalized parameters of the electron subsystem. The experimental values[17,28] of the lifetimes τ_l^e for excited states of chromophores BPEA, BDPY, and ZnPy: $\tau_{\text{BPEA}}^e = 2.82$ ns, $\tau_{\text{BDPY}}^e = 0.26$ ns, and $\tau_{\text{ZnPY}}^e = 0.45$ ns, respectively, can be achieved with the following set of coupling constants: $\alpha_{\text{BPEA}} \sim 10^{-7}$, $\alpha_{\text{BDPY}} \sim 10^{-6}$, and $\alpha_{\text{ZnPy}} \sim 7 \times 10^{-7}$.

IV. RESULTS AND DISCUSSIONS

Using Eqs. (B31) and (22) and two sets of parameters discussed in Sec. III, here we study electron and energy-transfer kinetics in the BPF complex with special emphasis on the femtosecond time range, where the effects of quantum coherence can play an important role. We consider both single- and double-exciton regimes.

A. Evolution of a single exciton in the BPF complex

In Fig. 2, we show the time evolution of the excited states populations provided that only the BPEA$_a$ chromophore is excited at $t = 0$ (single-exciton regime). We use here the parameter set I, where excitonic couplings are larger than reorganization energies (see Sec. III). The process starts with quantum beatings between the resonant BPEA$_a$ and BPEA$_b$ chromophores, with a decoherence time of the order of 100 fs (at $T = 300$ K). In a few picoseconds, the excitation energy is subsequently transferred to the adjacent BDPY moieties and to the ZnPy chromophores. Later on, an electron moves from the excited energy level of the porphyrins to the fullerene moiety, thus producing a charge-separated state, ZnPy$^+$–F$^-$, with a quantum yield 95%, which is in agreement with the experimental results.[16]

It is evident from Fig. 2 that excited state populations of the BDPY chromophores oscillate with much lower amplitudes and die out within a very short time, $t < 10$ fs, at both temperatures: $T = 300$ K and 77 K. The populations of the other sites of the BPF complex do not exhibit any oscillatory behavior. This can be ascribed to incoherent hopping becoming dominant because of significant energy mismatch between these chromophores.

Figure 3 shows the time dependence of the excited state populations of chromophores for the parameter set II, where the reorganization energies are larger than the excitonic cou-
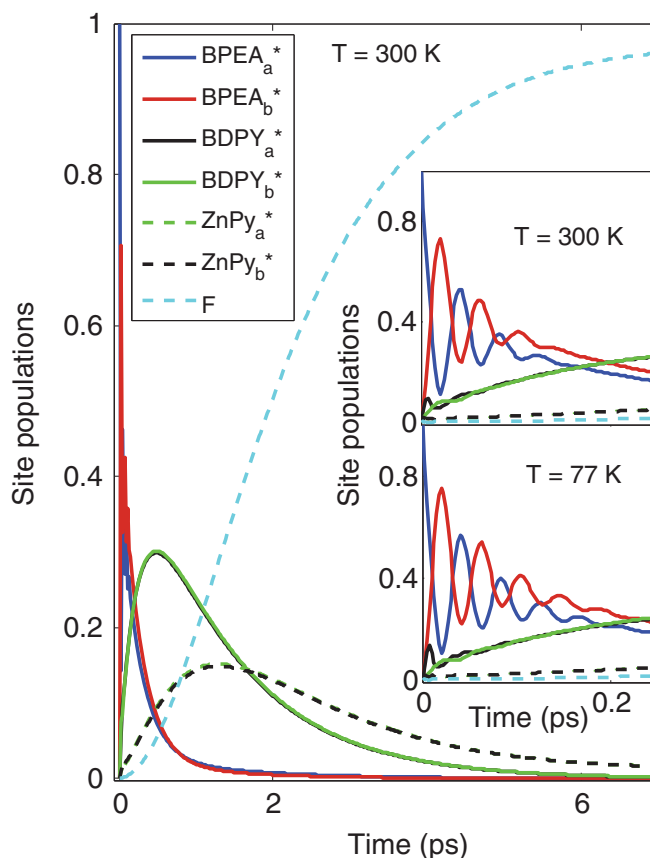

FIG. 2. Site populations as a function of time for the parameter set I. The inset plots depict the features of site populations for short time, at two different temperatures: $T = 300$ K and 77 K. The site populations of the BPEA moieties oscillate with a considerably large amplitude, while the oscillations of the other site populations are hardly observable.

plings between chromophores. At $t = 0$, the BPEA$_a$ chromophore is excited (single-exciton regime). Then, after a few picoseconds, the charge-separated state is formed with a quantum yield of the order of 97%. However, owing to a stronger system-environment coupling, quantum beats between the BPEA$_a$ and BPEA$_b$ chromophores have a lower amplitude and shorter decoherence time ($\sim$50 fs) than in the previous case when we used the parameter set I. We note that no quantum oscillations of the fullerene population (site F) are visible in Figs. 2 and 3.

No significant oscillations of the site populations were observed (not shown here) when the BDPY chromophores were initially (at $t = 0$) excited. In this case, due to the considerable energy gaps between the BDPY and the adjacent BPEA and ZnPy chromophores, incoherent hopping dominates over the coherent transfer of excitons. Furthermore, the structure of the BPF complex[15,28] does not allow direct energy transfer between two BDPY chromophores.

Figures 4 and 5 demonstrate the charge- and energy-transfer dynamics for two parameter sets, I and II, for the case when one of the porphyrin chromophores (ZnPy$_a$) is excited. Here, we do not show the time evolution of the BPEA and BDPY chromophores since these moieties have higher excitation energies than the ZnPy chromophore and they are not excited in the process. As evident from Figs. 4 and 5, the
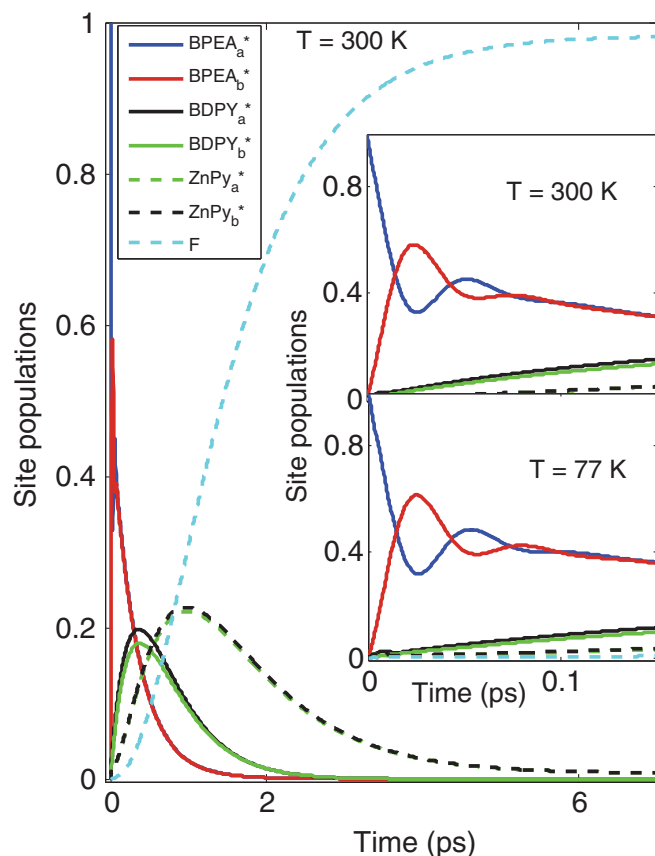
FIG. 3. This figure presents site populations as a function of time for the parameter set II. The inset plots show the site populations for short time, at two different temperatures: $T = 300$ K and 77 K. The amplitudes of the site-population oscillations are much smaller and die out earlier, compared to Fig. 2. This figure indicates that even for $\Lambda > V$, the energy transfer between BPEA chromophores is dominated by wave-like coherent motion.

FIG. 4. Site populations as a function of time for the parameter set I, when the $ZnPy_a$ chromophore is in the excited state and all the other chromophores are in the ground state at $t = 0$. The inset plots depict the site populations at short time for two temperatures: $T = 300$ K and 77 K. Lowering the temperature enhances the oscillations of the charge density on the fullerene moiety. Despite the huge energy difference between $ZnPy^*$-F and $ZnPy^+$-F^-, the charge of the fullerene site exhibits oscillatory behavior for short time, specially at lower temperatures.

excited porphyrin molecule rapidly transfers an electron to fullerene, thus producing a charge-separated state $ZnPy^+ - F^-$ with a quantum yield of about 98%. The most important feature here is that the population and charge of the fullerene molecule oscillates in time due to a quantum superposition of the porphyrin excited state and the state of an electron on the fullerene. The amplitude of these quantum beats is very small and the decoherence time is quite short ($\sim$10 fs at T = 77 K). This fact can be explained by the significant energy mismatch between the $ZnPy^* - F$ and $ZnPy^+ - F^-$ states as well as by the strong influence of the environment on the electron dynamics.

B. Evolution of double excitons in the BPF complex

In Sec. IV A, we consider a single exciton case with just one chromophore initially being in the upper energy state. Here we analyze a situation where two porphyrin molecules ($ZnPy_a$ and $ZnPy_b$) are excited at $t = 0$. Figures 6(a) and 6(b) show the coherent dynamics of the fullerene population (and the fullerene charge) for the parameter sets I (Fig. 6(a)) and II (Fig. 6(b)) at two different temperatures, $T = 77$ K and $T = 300$ K. We also compare the double-exciton case with the previously analyzed single-exciton case. It is apparent
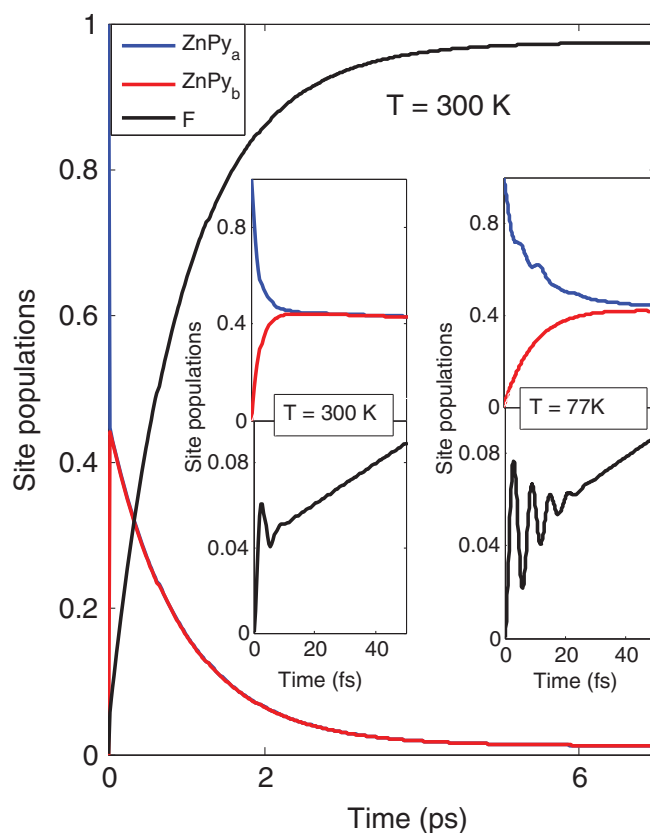
from Fig. 6 that the double excitation significantly enhances the amplitude of quantum oscillations of the fullerene charge for both sets of parameters. As one might expect, the frequency of the quantum beatings and the decoherence time are not affected by the number of excitons.

C. Amplification of charge oscillations

In the previous discussion we observed that lowering the temperature and the simultaneous excitation of both porphyrins significantly enhances quantum oscillations of the fullerene charge. In this subsection we show that these oscillations can also be controlled by tuning the following parameters:

1. Electron tunneling amplitude Δ

The electronic coupling between the fullerene electron acceptor and zinc porphyrins has a strong effect on the quantum oscillations of the fullerene charge. To explore this effect, in Fig. 7(a) we plot the electron population of the fullerene as a function of time, for different values of the coupling Δ. Figure 7(a) clearly shows that, with increasing Δ, the ampli-
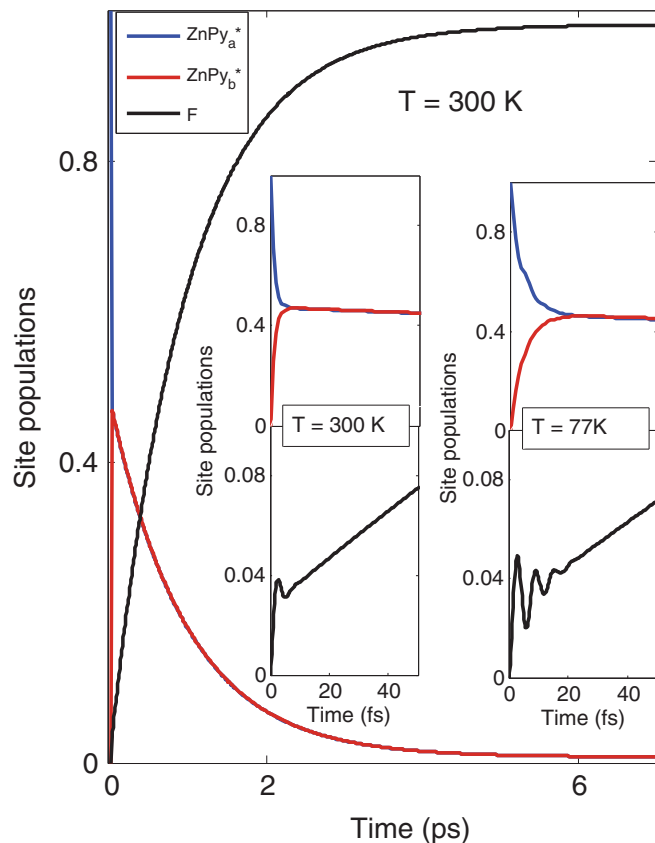
FIG. 5. Time evolution of the site populations for the parameter set II, starting with an exciton on the chromophore $ZnPy_a$ at $t = 0$. The inset plots depict the features of the site populations for a shorter time regime and at two temperatures: $T = 300$ K and 77 K. Lowering the temperature enhances oscillations of the charge density on the fullerene derivative. These results indicate that the population of the site F oscillates for short time, even for $\Lambda > V$. These oscillations are more pronounced at lower temperatures.

tude of the charge oscillations is significantly enhanced. This coupling can be increased by attaching the fullerene to porphyrins with better ligands which form much stronger covalent bonds.

2. Energy of the charge-separated state E_{ch}

The energy, $E_{ch} \sim 1370$ meV, of the charge-separated state, $ZnPy^+ - F^-$, is much lower than the energy of the zinc porphyrin excited state, $E_{ZnPy^*} \sim 2030$ meV. It is evident from Fig. 7(b) that increasing the energy E_{ch}, which leads to a decrease of the porpyrin-fullerene energy mismatch, results in a pronounced amplification of the quantum oscillations of the fullerene charge. The energy of the fullerene can be changed by placing nearby a charge residue, electrostatically coupled to the fullerene.

3. Reorganization energy λ_F

In Fig. 7(c) we present the time evolution of the fullerene population for different values of charge-transfer reorganization energy λ_F. This parameter can be decreased by replacing the polar solvent with another one which has a much lower polarity. As can be seen from Fig. 7(c), the quantum
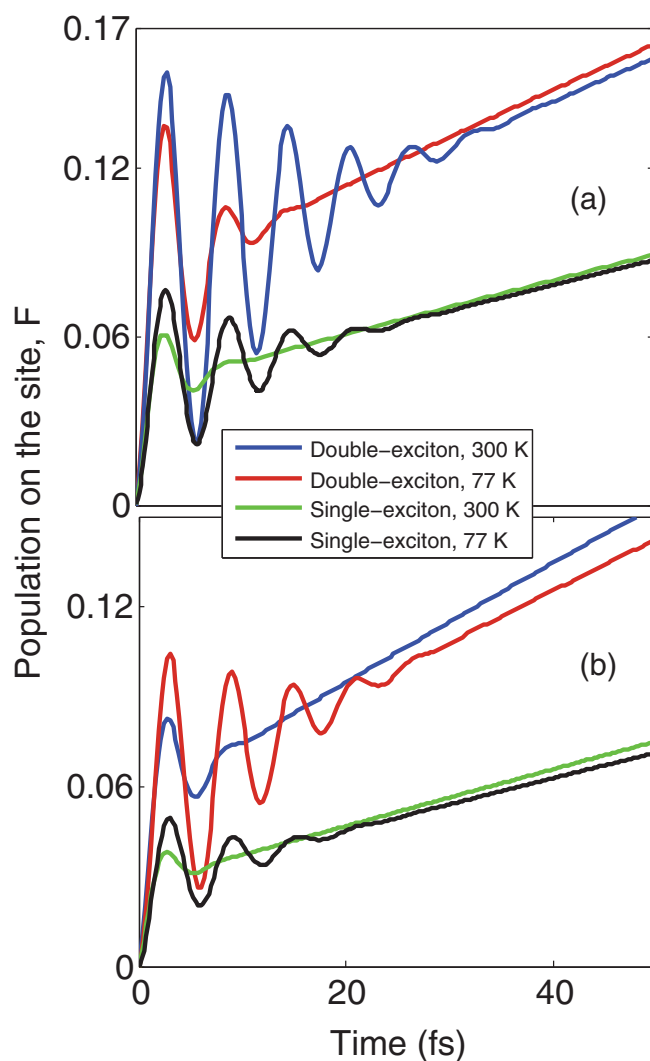

FIG. 6. Time evolution of the populations on the site F, for both sets of parameters, I and II, comparing the double-exciton case (the two ZnPy chromophores are excited) with the single-exciton case. (a) Time evolution of the populations on the site F for the parameter set I. (b) Time evolution of the populations on the site F for the parameter set II. Note that the double-excitation significantly enhances the amplitude of the charge oscillations at the fullerene site for both sets of parameters, either at low or at high temperatures.

oscillations of the fullerene charge survive much longer times for smaller values of the reorganization energy, which correspond to weaker system-environment couplings. A similar effect is expected when the porphyrin reorganization energy is changed.

V. CONCLUSIONS

We theoretically studied the energy and electron-transfer dynamics in a wheel-shaped artificial antenna-reaction center complex. This complex,[17] mimicking a natural photosystem, contains six chromophores ($BPEA_a$, $BPEA_b$, $BDPY_a$, $BDPY_b$, $ZnPy_a$, and $ZnPy_b$) and an electron acceptor (fullerene, F). Using the methods of dissipative quantum mechanics we derive and solve a set of equations for both the diagonal and off-diagonal elements of the density matrix, which describe quantum coherent effects in energy and charge
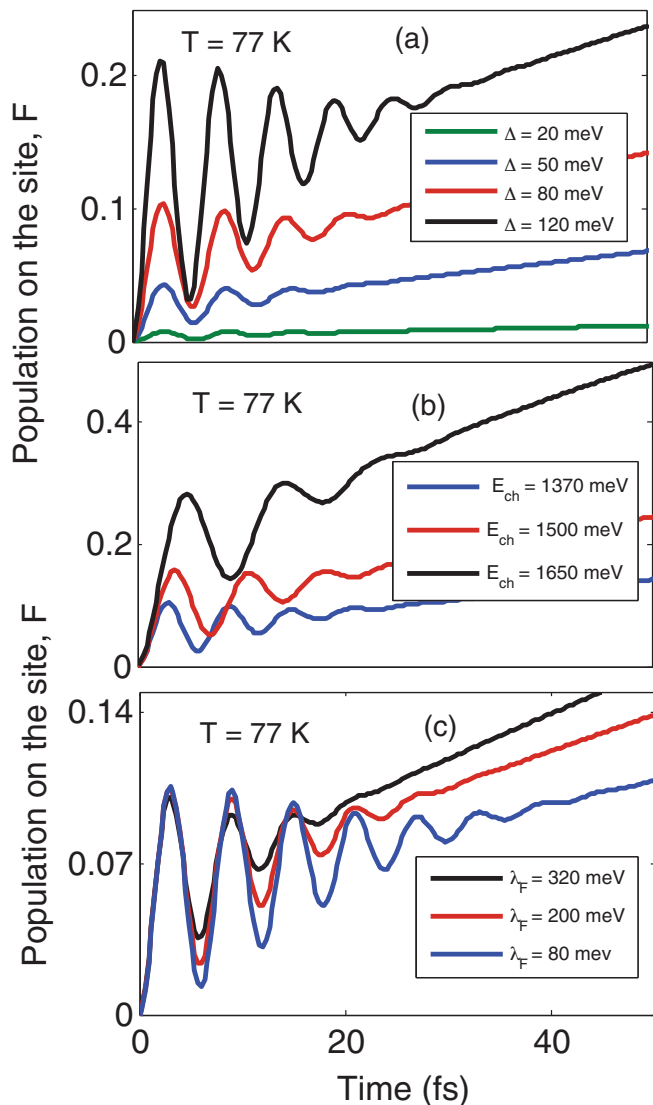
FIG. 7. Time evolution of the population on the site F for the parameter set II when both ZnPy chromophores are excited at $t = 0$. (a) Effects of the coupling Δ on the time evolution of the populations on the site F. (b) Effects of the energy gap between an excited state of a ZnPy chromophore and the charge-separated state, E_{ch}, on the time evolution of populations on the site F. (c) Effects of the reorganization energy λ on the time evolution of populations on the site F. As can be seen from these plots, the contribution of wave-like coherent motion to electron-transfer dynamics is significantly enhanced when strengthening the coupling between fullerene and porphyrin, lowering the energy gap between the fullerene and porphyrin sites, and decreasing the reorganization energy.

transfer. We consider two sets of parameters, one corresponding to the case where the energy-transfer reorganization energy Λ is less than the resonant coupling V between the chromophores, $\Lambda < V$, and another regime where $\Lambda > V$. For these two sets of parameters, we examine the electron and exciton dynamics, with special emphasis on the short-time regime ($\sim$ femtoseconds). We demonstrate that, in agreement with the experiments performed in Ref. 17, the excitation energy of the BPEA antenna chromophores is efficiently funneled to porphyrins (ZnPy). The excited ZnPy molecules rapidly donate an electron to the fullerene electron acceptor, thus creating a charge-separated state, $ZnPy^+ - F^-$, with a quantum yield of the order of 95%. There is no observable

difference in energy transduction efficiency for these two sets of parameters. In the limit of strong interchromophoric coupling, coherent dynamics dominates over incoherent-hopping motion. In the single-exciton regime, when one of the BPEA chromophores is initially excited, quantum beatings between two resonant BPEA chromophores occur with decoherence times of the order of 100 fs. However, here the electron transfer process is dominated by incoherent hopping. For the case where one porphyrin molecule is excited at the beginning, we obtain small quantum oscillations of the fullerene charge characterized by a short decay time scale ($\sim$10 fs). More pronounced quantum oscillations of the fullerene charge (with an amplitude $\sim$0.1 electron charge and decoherence time of about 20 fs at $T = 77$ K) are predicted for the double-exciton regime, when both porphyrin molecules are initially excited. We also show that the contribution of wave-like coherent motion to electron-transfer dynamics could be enhanced by lowering the temperature, strengthening the fullerene-porphyrin bonds, shrinking the energy gap between the zinc porphyrin and fullerene moieties (e.g., by attaching a charged residue to the fullerene), as well as by decreasing the reorganization energy (by tuning the solvent polarity).

APPENDIX A: COULOMB INTERACTION ENERGIES

The Coulomb interactions between the electron states are

$$H_C = -u_F[(1 - \bar{n}_{ZnPy_a})n_F + (1 - \bar{n}_{ZnPy_b})n_F]$$
$$+ u_{Py}(1 - \bar{n}_{ZnPy_a})(1 - \bar{n}_{ZnPy_b})$$
$$+ u_{ZnPy_a}n_{ZnPy_a}n_{ZnPy_a^*} + u_{ZnPy_b}n_{ZnPy_b}n_{ZnPy_b^*}, \quad (A1)$$

where

$$\bar{n}_{ZnPy_a} = n_{ZnPy_a} + n_{ZnPy_a^*} \quad \text{and} \quad \bar{n}_{ZnPy_b} = n_{ZnPy_b} + n_{ZnPy_b^*}.$$

The first term of Eq. (A1) represents the electrostatic attraction (so the minus sign) between the positively charged ZnPy chromophores and the negatively charged fullerene. The second term is due to the Coulomb repulsion (so the plus sign) between two ZnPy chromophores. The last two terms are the repulsive interaction energies when both the excited and ground states of the ZnPy chromophores are occupied by electrons. The coefficients u_F, u_{Py}, u_{ZnPy_a}, and u_{ZnPy_a} represent the magnitudes of the electrostatic interactions and these are calculated using the Coulomb formula. We have assumed that the empty ZnPy chromophores ($n_{ZnPy} + n_{ZnPy^*} = 0$) have

positive charges and the acceptor state F becomes negatively charged when it is occupied by an electron.

APPENDIX B: DERIVATION OF EQUATIONS FOR THE MATRIX $\langle \rho_{\mu\nu} \rangle$

Our derivation of the equations for the matrix $\langle \rho_{\mu\nu} \rangle$ is based on the exact solution for the operator $\rho_{\mu\nu} = (|\mu\rangle\langle\nu|)(t)$ of the system influenced only by diagonal fluctuations of the bath. In this case the "system + bath" Hamiltonian has the form

$$H_{\text{diag}} = \sum_\mu E_\mu |\mu\rangle\langle\mu| + \sum_j \left(\frac{p_j^2}{2m_j} + \frac{m_j \omega_j^2 x_j^2}{2} \right)$$
$$- \sum_\mu \sum_j m_j \omega_j^2 \Lambda_j^\mu x_j |\mu\rangle\langle\mu|, \quad \text{(B1)}$$

where $\Lambda_j^\mu = \Lambda_j^{\mu\mu}$ [see Eq. (13)]. The time evolution of the exciton operators $\rho_{\mu\nu}$ is governed by the Heisenberg equation

$$i\dot{\rho}_{\mu\nu} = -\omega_{\mu\nu}\rho_{\mu\nu} + \sum_j m_j \omega_j^2 (\Lambda_j^\mu - \Lambda_j^\nu) x_j \rho_{\mu\nu}. \quad \text{(B2)}$$

It is possible to verify that the solution of Eq. (B2) is given by the equation

$$\rho_{\mu\nu}(t) = \exp[i\Omega_{\mu\nu}(t - t_0)] \times \exp\left[i \sum_j p_j(t)\left(\Lambda_j^\mu - \Lambda_j^\nu\right) \right]$$
$$\times \exp\left[-i \sum_j p_j(t_0)\left(\Lambda_j^\mu - \Lambda_j^\nu\right) \right] \rho_{\mu\nu}(t_0), \quad \text{(B3)}$$

where

$$\Omega_{\mu\nu} = \omega_{\mu\nu} - \sum_j \frac{m_j \omega_j^2}{2}\left[\left(\Lambda_j^\mu\right)^2 - \left(\Lambda_j^\nu\right)^2\right], \quad \text{(B4)}$$

and p_j is the Heisenberg operator of the dissipative environment. The evolution begins at time $t = t_0$. The diagonal operators $\rho_\mu = \rho_{\mu\mu}$ are constant, $\rho_\mu(t) = \rho_\mu(t_0)$, in the presence of a strong interaction with the diagonal operators of the protein environment.

For uncorrelated diagonal and off-diagonal environment operators, when $\langle Q_\alpha^{(0)}(t)\tilde{Q}_{\mu\nu}^{(0)}(t')\rangle = 0$, the contribution of the environment to the non-Markovian equation (20) consists of two parts:

$$\langle -i[\rho_{\mu\nu}, H_{e\text{-ph}}]_- \rangle = \langle -i[\rho_{\mu\nu}, H_{e\text{-ph}}^{\text{diag}}]_- \rangle$$
$$+ \langle -i[\rho_{\mu\nu}, H_{e\text{-ph}}^{\text{n-diag}}]_- \rangle. \quad \text{(B5)}$$

The diagonal elements, Q_μ, of the environment contribute to the first part,

$$\langle -i[\rho_{\mu\nu}, H_{e\text{-ph}}^{\text{diag}}]_- \rangle$$
$$= \int_0^t dt_1 \langle (Q_\mu^{(0)} - Q_\nu^{(0)})(t) Q_{\bar{\nu}}^{(0)}(t_1)\rangle\langle\rho_{\mu\nu}(t)\rho_{\bar{\nu}}(t_1)\rangle$$
$$- \int_0^t dt_1 \langle Q_{\bar{\nu}}^{(0)}(t_1)(Q_\mu^{(0)} - Q_\nu^{(0)})(t)\rangle\langle\rho_{\bar{\nu}}(t_1)\rho_{\mu\nu}(t)\rangle, \quad \text{(B6)}$$

whereas the second part is due to a contribution of the non-diagonal (abbreviated as n-diag in the super-index) operators, $\tilde{Q}_{\mu\nu}$,

$$\langle -i[\rho_{\mu\nu}, H_{e\text{-ph}}^{\text{n-diag}}]_- \rangle$$
$$= -\int_0^t dt_1 \langle \tilde{Q}_{\nu\alpha}^{(0)}(t) \tilde{Q}_{\bar{\mu}\bar{\nu}}^{(0)}(t_1)\rangle\langle\rho_{\mu\alpha}(t)\rho_{\bar{\mu}\bar{\nu}}(t_1)\rangle$$
$$+ \int_0^t dt_1 \langle \tilde{Q}_{\bar{\mu}\bar{\nu}}^{(0)}(t_1) \tilde{Q}_{\nu\alpha}^{(0)}(t)\rangle\langle\rho_{\bar{\mu}\bar{\nu}}(t_1)\rho_{\mu\alpha}(t)\rangle$$
$$+ \int_0^t dt_1 \langle \tilde{Q}_{\alpha\mu}^{(0)}(t) \tilde{Q}_{\bar{\mu}\bar{\nu}}^{(0)}(t_1)\rangle\langle\rho_{\alpha\nu}(t)\rho_{\bar{\mu}\bar{\nu}}(t_1)\rangle$$
$$- \int_0^t dt_1 \langle \tilde{Q}_{\bar{\mu}\bar{\nu}}^{(0)}(t_1) \tilde{Q}_{\alpha\mu}^{(0)}(t)\rangle\langle\rho_{\bar{\mu}\bar{\nu}}(t_1)\rho_{\alpha\nu}(t)\rangle. \quad \text{(B7)}$$

We note that the time evolution of the diagonal elements of the system operator, $\rho_\mu = \rho_{\mu\mu}$, is determined by the non-diagonal operators $\tilde{Q}_{\mu\nu}$ as well as by quenching terms. Strong diagonal fluctuations of the environment have no effect on the evolution of the diagonal elements of the matrix. Thus, in Eq. (B6) we assume $\rho_{\bar{\nu}}(t_1) = \rho_{\bar{\nu}}(t)$ so that Eq. (B6) can be rewritten as

$$\langle -i[\rho_{\mu\nu}, H_{e\text{-ph}}^{\text{diag}}]_- \rangle = -\left(\Gamma_{\mu\nu}^{\text{diag}} + i\delta\Omega_{\mu\nu}^{\text{diag}}\right)(t)\langle\rho_{\mu\nu}(t)\rangle, \quad \text{(B8)}$$

where the time-dependent rate, $\Gamma_{\mu\nu}^{\text{diag}}(t)$, and the frequency shift, $\delta\Omega_{\mu\nu}^{\text{diag}}$, can be found from the following expression:

$$\Gamma_{\mu\nu}^{\text{diag}}(t) + i\delta\Omega_{\mu\nu}^{\text{diag}}(t) = \int_0^t dt_1 \left\{ \langle (Q_\mu^{(0)} - Q_\nu^{(0)})(t) Q_\nu^{(0)}(t_1)\rangle \right.$$
$$\left. - \langle Q_\mu^{(0)}(t_1)(Q_\mu^{(0)} - Q_\nu^{(0)})(t)\rangle \right\}. \quad \text{(B9)}$$

The rate $\Gamma_{\mu\nu}^{\text{diag}}(t)$ determines the fast decay of quantum coherence in our system. For an environment composed of independent oscillators, we obtain

$$\langle (Q_\mu^{(0)} - Q_\nu^{(0)})(t) Q_\nu^{(0)}(t_1)\rangle - \langle Q_\mu^{(0)}(t_1)(Q_\mu^{(0)} - Q_\nu^{(0)})(t)\rangle$$
$$= -\sum_j \frac{m_j \omega_j^3}{2}\left(\Lambda_j^\mu - \Lambda_j^\nu\right)^2 \coth\left(\frac{\omega_j}{2T}\right)\cos\omega_j(t - t_1)$$
$$- i\sum_j \frac{m_j \omega_j^3}{2}\left[\left(\Lambda_j^\mu\right)^2 - \left(\Lambda_j^\nu\right)^2\right]\sin\omega_j(t - t_1). \quad \text{(B10)}$$

The fluctuations of the diagonal operators of the environment can be described by the set of spectral functions,

$$J_\mu(\omega) = \sum_j \frac{m_j \omega_j^3}{2}\left(\Lambda_j^\mu\right)^2 \delta(\omega - \omega_j),$$

$$\bar{J}_{\mu\nu}(\omega) = \sum_j \frac{m_j \omega_j^3}{2}\left(\Lambda_j^\mu - \Lambda_j^\nu\right)^2 \delta(\omega - \omega_j), \quad \text{(B11)}$$

together with the corresponding reorganization energies,

$$\lambda_\mu = \int_0^\infty \frac{d\omega}{\omega} J_\mu(\omega) = \sum_j \frac{m_j \omega_j^2}{2}\left(\Lambda_j^\mu\right)^2,$$

$$\bar{\lambda}_{\mu\nu} = \int_0^\infty \frac{d\omega}{\omega} \bar{J}_{\mu\nu}(\omega) = \sum_j \frac{m_j \omega_j^2}{2}\left(\Lambda_j^\mu - \Lambda_j^\nu\right)^2. \quad \text{(B12)}$$

We also introduce a spectral function, $\tilde{J}_{\mu\nu}(\omega)$, which characterizes the non-diagonal ($\mu \neq \nu$) environment fluctuations,

$$\tilde{J}_{\mu\nu}(\omega) = \sum_j \frac{m_j \omega_j^3}{2} |\tilde{\Lambda}_j^{\mu\nu}|^2 \delta(\omega - \omega_j), \qquad \text{(B13)}$$

where $\tilde{\Lambda}_j^{\mu\nu} = \Lambda_j^{\mu\nu}$ [see Eq. (13)] taken at $\mu \neq \nu$. With Eq. (B10) we calculate the contributions of the diagonal environment fluctuations into the decoherence rate and the frequency shift of the off-diagonal elements of the system matrix $\langle\rho_{\mu\nu}\rangle$ in Eq. (B8),

$$\Gamma_{\mu\nu}^{\text{diag}}(t) = \int_0^\infty \frac{d\omega}{\omega} \bar{J}_{\mu\nu}(\omega) \coth\left(\frac{\omega}{2T}\right) \sin\omega t,$$

$$\delta\Omega_{\mu\nu}^{\text{diag}}(t) = \int_0^\infty \frac{d\omega}{\omega} [J_\mu(\omega) - J_\nu(\omega)](1 - \cos\omega t). \quad \text{(B14)}$$

The contribution of the non-diagonal fluctuations of the environment to the evolution of the electron operators $\langle\rho_{\mu\nu}\rangle$ is defined by Eq. (B7). To calculate the products of exciton variables taken at different moments of time, for example, $\rho_{\mu\alpha}(t)\rho_{\bar{\mu}\bar{\nu}}(t_1)$, we use Eq. (B3), which describes the evolution of exciton operators in the presence of strong coupling to the diagonal operators, Q_μ, of the environment. We assume that the interaction with the non-diagonal environment operators, $\tilde{Q}_{\mu\nu}$, is weak. With Eq. (B3) we express the operators at time t_1 in terms of operators taken at time t:

$$\rho_{\bar{\mu}\bar{\nu}}(t_1) = \exp[-i\Omega_{\bar{\mu}\bar{\nu}}\tau]$$
$$\times \exp[iu_{\bar{\mu}\bar{\nu}}(\tau)]\exp[-iv_{\bar{\mu}\bar{\nu}}(t,t_1)]\rho_{\mu\nu}(t), \rho_{\bar{\mu}\bar{\nu}}(t_1)$$
$$= \rho_{\mu\nu}(t)\exp[-i\Omega_{\bar{\mu}\bar{\nu}}\tau]\exp[-iu_{\bar{\mu}\bar{\nu}}(\tau)]$$
$$\times \exp[-iv_{\bar{\mu}\bar{\nu}}(t,t_1)], \qquad \text{(B15)}$$

where $\tau = t - t_1$, and

$$u_{\mu\nu}(\tau) = \int_0^\infty \frac{d\omega}{\omega} \bar{J}_{\mu\nu}(\omega) \sin\omega\tau,$$

$$v_{\mu\nu}(t,t_1) = \sum_j \left(\Lambda_j^\mu - \Lambda_j^\nu\right)[p_j(t) - p_j(t_1)]. \quad \text{(B16)}$$

Here, we assume that $p_j(t)$, $p_j(t_1)$ are free-evolving momentum operators of the environment, which are described by Gaussian statistics with a correlation function

$$\left\langle \frac{1}{2}[\,p_j(t), p_j(t_1)]_+\right\rangle = \frac{\hbar m_j \omega_j}{2} \coth\left(\frac{\hbar\omega_j}{2T}\right) \cos\omega_j(t - t_1). \tag{B17}$$

The operator function $v_{\mu\nu}(t,t_1)$ does not commute with the exciton matrix $\rho_{\mu\nu}(t)$, and, therefore, we need two expressions for the operator $\rho_{\mu\nu}(t_1)$, which are distinguished by the order of the operators $\rho_{\mu\nu}(t)$ and $\exp[-iv_{\mu\nu}(t,t_1)]$. For the average value of the operator $\exp[-iv_{\mu\nu}(t,t_1)]$, we obtain

$$\langle\exp[-iv_{\mu\nu}(t,t_1)]\rangle$$
$$= \exp\left\{-\int_0^\infty \frac{d\omega}{\omega^2} \bar{J}_{\mu\nu}(\omega) \coth\left(\frac{\hbar\omega}{2T}\right)[1 - \cos\omega(t-t_1)]\right\}. \tag{B18}$$

Substituting Eq. (B15) into Eq. (B7) and using the secular approximation, we obtain a contribution of the non-diagonal

environment operators, $\tilde{Q}_{\mu\nu}$, to the evolution of diagonal exciton operators $\langle\rho_\mu\rangle$,

$$\langle -i[\rho_\mu, H_{e\text{-ph}}^{\text{n-diag}}]_-\rangle = -\sum_\alpha \tilde{\gamma}_{\alpha\mu}(t)\langle\rho_\mu\rangle + \sum_\alpha \tilde{\gamma}_{\mu\alpha}(t)\langle\rho_\alpha\rangle, \tag{B19}$$

characterized by the following relaxation matrix:

$$\tilde{\gamma}_{\mu\alpha}(t)$$
$$= \int_0^t dt_1 \langle\tilde{Q}_{\alpha\mu}^{(0)}(t)\tilde{Q}_{\mu\alpha}^{(0)}(t_1)\rangle e^{-i\Omega_{\mu\alpha}(t-t_1)} e^{-iu_{\mu\alpha}(t-t_1)} \langle e^{-iv_{\mu\alpha}(t,t_1)}\rangle$$
$$+ \int_0^t dt_1 \langle\tilde{Q}_{\alpha\mu}^{(0)}(t_1)\tilde{Q}_{\mu\alpha}^{(0)}(t)\rangle e^{-i\Omega_{\alpha\mu}(t-t_1)} e^{iu_{\alpha\mu}(t-t_1)} \langle e^{-iv_{\alpha\mu}(t,t_1)}\rangle, \tag{B20}$$

where

$$\langle\tilde{Q}_{\alpha\mu}^{(0)}(t)\tilde{Q}_{\mu\alpha}^{(0)}(t_1)\rangle = (1/2)\int_0^\infty \tilde{J}_{\alpha\mu}(\omega)$$
$$\times \left\{\left[\coth\left(\frac{\omega}{2T}\right) - 1\right]e^{i\omega(t-t_1)}\right.$$
$$\left. + \left[\coth\left(\frac{\omega}{2T}\right) + 1\right]e^{-i\omega(t-t_1)}\right\}. \tag{B21}$$

When the environment is at high temperatures ($2T \gg \omega$) and at low frequencies of the diagonal fluctuations ($\omega\tau \ll 1$), we have

$$u_{\mu\nu}(\tau) \simeq \bar{\lambda}_{\mu\nu}\tau,$$

and

$$\langle\exp[-iv_{\mu\nu}(t,t_1)]\rangle \simeq \exp[-\bar{\lambda}_{\mu\nu}T(t-t_1)^2].$$

With these assumptions the relaxation matrix has a simple form

$$\tilde{\gamma}_{\mu\alpha} = \sqrt{\frac{\pi}{\bar{\lambda}_{\alpha\mu}}} \int_0^\infty d\omega \, \tilde{J}_{\alpha\mu}(\omega)\, n(\omega)$$
$$\times \left\{ \exp\left[-\frac{(\omega + \Omega_{\alpha\mu} - \bar{\lambda}_{\alpha\mu})^2}{4\bar{\lambda}_{\alpha\mu}T}\right] \right.$$
$$\left. + \exp\left(\frac{\omega}{T}\right)\exp\left[-\frac{(\omega - \Omega_{\alpha\mu} + \bar{\lambda}_{\alpha\mu})^2}{4\bar{\lambda}_{\alpha\mu}T}\right]\right\}, \tag{B22}$$

where $n(\omega) = [\exp(\omega/T) - 1]^{-1}$ is the Bose distribution function at the temperature T. The moment of time t in the expression (B20) for the relaxation matrix is usually higher than the effective retardation time, $\tau_c \sim (\bar{\lambda}_{\alpha\mu}T)^{-1/2}$, of the integrand in Eq. (B20): $t \gg \tau_c$. Therefore, we assume that $t \simeq \infty$ so that $\tilde{\gamma}_{\mu\alpha}(t) \simeq \tilde{\gamma}_{\mu\alpha}(\infty) = \tilde{\gamma}_{\mu\alpha}$.

It follows from Eq. (B7) that a contribution of the non-diagonal environment operators $\tilde{Q}_{\mu\nu}$ to the evolution of the off-diagonal elements $\rho_{\mu\nu}$ is given by the formula

$$\langle -i[\rho_{\mu\nu}, H_{e\text{-ph}}^{\text{n-diag}}]_-\rangle = -(\tilde{\Gamma}_{\mu\nu} + i\delta\tilde{\Omega}_{\mu\nu})(t)\langle\rho_{\mu\nu}(t)\rangle, \tag{B23}$$

where

$$
\tilde{\Gamma}_{\mu\nu}(t) + i\delta\tilde{\Omega}_{\mu\nu}(t)
$$

$$
= \int_0^t dt_1 \langle \tilde{Q}_{\nu\alpha}^{(0)}(t)\tilde{Q}_{\alpha\nu}^{(0)}(t_1)\rangle e^{-i\Omega_{\alpha\nu}(t-t_1)} e^{-iu_{\alpha\nu}(t-t_1)} \langle e^{-iv_{\alpha\nu}(t,t_1)}\rangle
$$

$$
+ \int_0^t dt_1 \langle \tilde{Q}_{\mu\alpha}^{(0)}(t)\tilde{Q}_{\alpha\mu}^{(0)}(t_1)\rangle e^{-i\Omega_{\mu\alpha}(t-t_1)} e^{iu_{\mu\alpha}(t-t_1)} \langle e^{-iv_{\mu\alpha}(t,t_1)}\rangle.
$$

(B24)

A small frequency shift, $\delta\tilde{\Omega}_{\mu\nu}$, can be hereafter ignored. The dephasing rate, $\tilde{\Gamma}_{\mu\nu}$, has two parts, $\tilde{\Gamma}_{\mu\nu} = \tilde{\Gamma}_\mu + \tilde{\Gamma}_\nu$, where

$$
\tilde{\Gamma}_\mu = \frac{1}{2}\sum_\alpha \sqrt{\frac{\pi}{\bar{\lambda}_{\mu\alpha}T}} \int_0^\infty d\omega \tilde{J}_{\mu\alpha}(\omega)n(\omega)
$$

$$
\times \left\{ \exp\left[-\frac{(\omega + \Omega_{\mu\alpha} - \bar{\lambda}_{\mu\alpha})^2}{4\bar{\lambda}_{\mu\alpha}T} \right] \right.
$$

$$
\left. + \exp\left(\frac{\omega}{T}\right)\exp\left[-\frac{(\omega - \Omega_{\mu\alpha} + \bar{\lambda}_{\mu\alpha})^2}{4\bar{\lambda}_{\mu\alpha}T} \right] \right\}.
$$

(B25)

We note that $\tilde{\Gamma}_\mu = (1/2)\sum_\alpha \tilde{\gamma}_{\alpha\mu}$, and $\Omega_{\mu\nu} = \omega_{\mu\nu} - \lambda_\mu + \lambda_\nu$ from Eqs. (B4) and (B12).

Assuming that the environment fluctuations acting on each electron-binding site are independent and using Eq. (13) for the coefficients $\Lambda_j^{\mu\nu}$, we obtain

$$
\tilde{J}_{\mu\nu}(\omega) = \sum_l [J_{lS}(\omega)|\langle\mu|S_l|\nu\rangle|^2 + J_{lM}(\omega)|\langle\mu|M_l|\nu\rangle|^2]
$$

$$
+ J_F(\omega)|\langle\mu|n_F|\nu\rangle|^2,
$$

(B26)

where

$$
J_{lS}(\omega) = \sum_j \frac{m_j\omega_j^3}{2}\bar{x}_{jl}^2\delta(\omega - \omega_j),
$$

$$
J_{lM}(\omega) = \sum_j \frac{m_j\omega_j^3}{2}\tilde{x}_{jl}^2\delta(\omega - \omega_j),
$$

$$
J_F(\omega) = \sum_j \frac{m_j\omega_j^3}{2}x_{jF}^2\delta(\omega - \omega_j).
$$

(B27)

The results obtained above are valid for an arbitrary frequency dependence of the spectral densities $J_{lS}(\omega)$, $J_{lM}(\omega)$, and $J_F(\omega)$. Hereafter we assume that these functions are described by the Lorentz–Drude formula characterized by a common inverse correlation time, $\gamma_c = \tau_c^{-1}$, and by a corresponding reorganization energy λ_{lS}, λ_{lM}, or λ_F, e.g.,

$$
J_{lS}(\omega) = 2\frac{\lambda_{lS}}{\pi}\frac{\omega\gamma_c}{\omega^2 + \gamma_c^2}.
$$

(B28)

Quenching processes also contribute to the decay of the off-diagonal elements, $\langle\rho_{\mu\nu}\rangle$, with the following decoherence rates: $\Gamma_{\mu\nu}^{\text{quen}} = \Gamma_\mu^{\text{quen}} + \Gamma_\nu^{\text{quen}}$, where

$$
\Gamma_\mu^{\text{quen}} = \sum_{l\alpha} |\langle\mu|a_l^\dagger a_{l*}|\alpha\rangle|^2 \chi_l''(\omega_{\mu\alpha})\left[\coth\left(\frac{\omega_{\mu\alpha}}{2T}\right) + 1\right].
$$

(B29)

Here, we consider an Ohmic quenching heat bath with the spectral density $\chi_l''(\omega) = \alpha_l\omega$, which is determined by a set of site-dependent dimensionless coupling constants $\alpha_l \ll 1$. The contribution of quenching to the relaxation of the diagonal elements of the electron matrix, $\langle\rho_\mu\rangle$, is determined by the standard Redfield term

$$
\gamma_{\mu\nu}^{\text{quen}} = \sum_l (|\langle\mu|a_l^\dagger a_{l*}|\nu\rangle|^2 + |\langle\nu|a_l^\dagger a_{l*}|\mu\rangle|^2)\chi_l''(\omega_{\mu\nu})
$$

$$
\times \left[\coth\left(\frac{\omega_{\mu\nu}}{2T}\right) - 1\right].
$$

(B30)

As a result, we find that the time evolution of the off-diagonal elements of the electron matrix is determined by the expression

$$
\langle\rho_{\mu\nu}\rangle(t) = \exp(i\omega_{\mu\nu}t - \bar{\lambda}_{\mu\nu}Tt^2) \times \exp(-\Gamma_{\mu\nu}t)\rho_{\mu\nu}(0),
$$

(B31)

with the decoherence rates $\Gamma_{\mu\nu} = \Gamma_\mu + \Gamma_\nu$, where the coefficient Γ_μ contains contributions of the off-diagonal fluctuations of the environment (Eq. (B25)) as well as quenching processes Γ_μ^{quen} (Eq. (B29)): $\Gamma_\mu = \tilde{\Gamma}_\mu + \Gamma_\mu^{\text{quen}}$. The evolution starts at the moment $t = 0$ with the initial matrix $\rho_{\mu\nu}(0)$. An effect of diagonal environment fluctuations is determined by the rate $\sqrt{\bar{\lambda}_{\mu\nu}T}$, where $\bar{\lambda}_{\mu\nu}$ is the reorganization energy defined by Eq. (B12) and T is the temperature of the environment.

[1]R. E. Blankenship, *Molecular Mechanisms of Photosynthesis* (Blackwell Science, Oxford, UK, 2002).

[2]H. V. Amerongen, L. Valkunas, and R. van Grondelle, *Photosynthetic Excitons* (World Scientific, Singapore, 2000).

[3]G. S. Engel, T. R. Calhoun, E. L. Read, T. K. Ahn, T. Mančal, Y. C. Cheng, R. E. Blankenship, and G. R. Fleming, Nature (London) **446**, 782 (2007).

[4]G. Panitchayangkoon, D. Hayes, K. A. Fransted, J. R. Caram, E. Harel, J. Wen, R. E. Blankenship, and G. S. Engel, Proc. Natl. Acad. Sci. U.S.A. **107**, 12766 (2010).

[5]P. Rebentrost, M. Mohseni, I. Kassal, S. Lloyd, and A. Aspuru-Guzik, New J. Phys. **11**, 033003 (2009); P. Rebentrost, R. Chakraborty, and A. Aspuru-Guzik, J. Chem. Phys. **131**, 184102 (2009).

[6]M. B. Plenio and S. F. Huelga, New J. Phys. **10**, 113019 (2008).

[7]A. Ishizaki and G. R. Fleming, Proc. Natl. Acad. Sci. U.S.A. **106**, 17255 (2009).

[8]Y.-C. Cheng and G. R. Fleming, Annu. Rev. Phys. Chem. **60**, 241 (2009).

[9]M. Sarovar, A. Ishizaki, G. R. Fleming, and K. B. Whaley, Nat. Phys. **6**, 462 (2010).

[10]E. Collini and G. D. Scholes, Science **323**, 369 (2009).

[11]J. Barber, Chem. Soc. Rev. **38**, 185 (2009).

[12]A. W.D. Larkum, Curr. Opin. Biotechnol. **21**, 271 (2010).

[13]G. Steinberg-Yfrach, P. A. Liddell, S. C. Hung, A. L. Moore, D. Gust, and T. A. Moore, Nature (London) **385**, 239 (1997).

[14]G. Steinberg-Yfrach, J. L. Rigaud, E. N. Durantini, A. L. Moore, D. Gust, and T. A. Moore, Nature (London) **392**, 479 (1998).

[15]G. Kodis, Y. Terazono, P. A. Liddell, J. Andréasson, V. Garg, H. Hambourger, T. A. Moore, A. L. Moore, and D. Gust, J. Am. Chem. Soc. **128**, 1818 (2006).

[16]D. Gust, T. A. Moore, and A. L. Moore, Acc. Chem. Res. **42**, 1890 (2009).

[17]Y. Terazono, G. Kodis, P. A. Liddell, V. Garg, T. A. Moore, A. L. Moore, and D. Gust, J. Phys. Chem. B **113**, 7147 (2009).

[18] H. Imahori, H. Yamada, Y. Nishimura, I. Yamazaki, and Y. Sakata, J. Phys. Chem. B **104**, 2099 (2000).

[19] P. K. Ghosh, A. Yu. Smirnov, and F. Nori, J. Chem. Phys. **131**, 035102 (2009).

[20] A. Yu. Smirnov, L. G. Mourokh, P. K. Ghosh, and F. Nori, J. Phys. Chem. C **113**, 21218 (2009).

[21] A. J. Leggett, S. Chakravarty, A. T. Dorsey, M. P. A. Fisher, A. Garg, and W. Zwerger, Rev. Mod. Phys. **59**, 1 (1987).

[22] A. Yu. Smirnov, L. G. Mourokh, and F. Nori, J. Chem. Phys. **130**, 235105 (2009).

[23] Y. Tanimura, J. Phys. Soc. Jpn. **75**, 082001 (2006).

[24] G. F. Efremov and A. Yu. Smirnov, Sov. Phys. JETP **53**, 547 (1981); G. F. Efremov, L. G. Mourokh, and A. Yu. Smirnov, Phys. Lett. A **175**, 89 (1993); A. Yu. Smirnov, Phys. Rev. B **68**, 134514 (2003).

[25] A. Ishizaki and G. R. Fleming, J. Chem. Phys. **130**, 234111 (2009).

[26] W. M. Zhang, T. Meier, V. Chernyak, and S. Mukamel, J. Chem. Phys. **108**, 7763 (1998).

[27] M. Yang and G. R. Fleming, Chem. Phys. **282**, 163 (2002).

[28] Y. Terazono, G. Kodis, P. A. Liddell, V. Garg, M. Gervaldo, T. A. Moore, A. L. Moore, and G. Gust, Photochem. Photobiol. **83**, 464–469 (2007).